AIP Conference Proceedings

Electrochemical synthesis of nanowires electrodes and their application in energy storage devices

Cite as: AIP Conference Proceedings **2145**, 020012 (2019); https://doi.org/10.1063/1.5123573
Published Online: 27 August 2019

Pier Giorgio Schiavi, Luca Farina, Antonio Rubino, Pietro Altimari, Maria Assunta Navarra, Robertino Zanoni, Stefania Panero, and Francesca Pagnanelli

View Online Export Citation

ARTICLES YOU MAY BE INTERESTED IN

Ti/TiO_2/Cu_2O electrodes for photocatalytic applications: Synthesis and characterization
AIP Conference Proceedings **2145**, 020005 (2019); https://doi.org/10.1063/1.5123566

Cu-catalyzed Si-NWs grown on "carbon paper" as anodes for Li-ion cells
AIP Conference Proceedings **2145**, 020010 (2019); https://doi.org/10.1063/1.5123571

Synthesis of fluorescent silver nanoclusters with potential application for heavy metal ions detection in water
AIP Conference Proceedings **2145**, 020007 (2019); https://doi.org/10.1063/1.5123568

© 2019 Author(s).

Electrochemical Synthesis of Nanowires Electrodes and their Application in Energy Storage Devices

Pier Giorgio Schiavi[1, a)], Luca Farina[1], Antonio Rubino[1], Pietro Altimari[1], Maria Assunta Navarra[1], Robertino Zanoni[1], Stefania Panero[1] and Francesca Pagnanelli[1]

[1]*Department of Chemistry, Sapienza University of Rome, P.le A. Moro 00185 Rome (IT)*
[a)] Corresponding author: piergiorgio.schiavi@uniroma1.it

Abstract. In this work, an electrochemical approach to synthesize Metal-MetalOxide/Hydroxide core-shell nanowires electrodes (NWE) is illustrated. NWE electrodes were obtained by electrodeposition of a targeted metal into the nanopores of nanoporous alumina templates generated by one-step anodization of aluminum. Following metal electrodeposition, the alumina template was selectively etched to obtain an array of free-standing metal nanowires. The imposed electrodeposition conditions allowed directly attaining a core-shell nanostructure, with a metal core covered by a thin metal oxide/hydroxide film. NWE electrodes produced by the proposed synthesis route were tested for the application as electrodes in lithium batteries and supercapacitors. To this purpose, an array of cobalt nanowires (CoNWs) supported by a nanostructured copper current collector was produced by sequential electrodeposition of cobalt and copper, and it was employed as anode in a lithium battery, while a NWE based on Ni-NiO/OH_2 (NiNWs) was obtained by nickel electrodeposition and tested as electrode in a supercapacitor. A thorough analysis and characterization of the produced electrodes were performed. The experiments with the lithium cell evidenced the positive effect of metallic core on stability, while the electrochemical characterization of the supercapacitor showed the presence of both NiO and $NiOH_2$ leading, when cycled, to a capacity close to the best literature value.

INTRODUCTION

The gradual replacement of fossil fuels with renewable sources and the rapidly increasing demand of mobile electronic devices and electric vehicles make it necessary the development of new highly performing energy storage systems. Lithium ion batteries and supercapacitors are the most promising storage devices due to their fast charge–discharge rate, long cycle life, high power and energy density[1]. Many efforts are currently focused on the development of new materials to apply in lithium ion batteries and supercapacitors. In this framework, considerable interest has been attracted by nanostructured transition metals oxides characterized by high theoretical specific capacity but with low electronic conductivity not allowing fast electron transport needed in high rates application. Several studies demonstrated as an inactive metallic core can improve electronic conductivity and cycling stability [2, 3]. Among various nanomaterials, nanowires structured electrode can be a promising solution. Besides the great surface area, nanowires structured electrodes can avoid morphology and surface change during battery or supercapacitor cycling. In fact, this nanoporous structure shows buffer properties towards the volume expansion taking place during oxidation and reduction of transition metals oxides that occur during the cycling the storage devices [4]. Two main routes can be followed to produce nanowires-based electrode (NWE): hydrothermal synthesis and template electrodeposition. By hydrothermal synthesis, the nanowire length and aspect ratio are poorly controlled and a separate reduction stage is required to generate a metallic core. On the other hand, template electrodeposition allows effectively controlling nanowire length and aspect ratio, but it involves the application of membranes generated by double-step anodization of aluminum and their coating by sputter metal deposition [5, 6]. These latter characteristics hinder the scale-up of the template electrodeposition process. In the present work, a versatile method is proposed to produce nanowires-based electrodes overcoming the illustrated technological limits. Furthermore, the imposed electrodeposition conditions allow directly attaining a core-shell nanostructure with a metallic nanowires core.

NANOINNOVATION 2018
AIP Conf. Proc. 2145, 020012-1–020012-7; https://doi.org/10.1063/1.5123573
Published by AIP Publishing. 978-0-7354-1890-5/$30.00

MATERIALS AND METHODS

Electrodes synthesis and characterization

Metal electrodeposition into nanoporous alumina templates was performed as reported in our previous work [7-9]. Briefly, alumina templates were obtained by anodization of aluminium foils (Alfa Aesar 99% - 1% Si + Fe, 0.25 mm thickness). The employed aluminium foil was electropolished with a solution of 1:4 $HClO_4$ 60%wt : CH_3CH_2OH before each anodization Both electropolishing and anodization tests were performed in a two-electrode jacketed cell with a constant temperature of 0.0 ± 0.2 °C. Anodic alumina oxide (AAO) templates were produced by one-step anodization in a 0.3 M H_2SO_4 solution with an applied potential of 25 V for a duration of 90 min. As well known, a barrier oxide layer at the bottom of each pore characterizes any template produced by aluminium anodization. The barrier layer has high electrical resistance and thus electrically isolates the underlying aluminium from the electrodeposition bath. A decrease in the barrier layer resistance was achieved by a decrement of the anodization applied potential. The decrease of the anodization potential decrease the aluminium oxide formation, while, the dissolution rate, of the formed aluminum oxide through the acidic electrolyte solution, was kept constant. The effect of this treatment results in a dissolution of the oxide layer at the bottom of each nanopores [10]. In order to improve the electrical conductivity of the alumina template, at the end of any anodization, the cell potential was step-wise decreased every 30 seconds.

Nanowire electrodeposition tests were performed in a magnetically stirred three electrode jacketed glass cell at constant temperature of 35.0 ± 0.2 °C. Ag/AgCl saturated electrode, 25x20 mm Pt gauze and the AAO template were the reference, counter and the working electrode, respectively. The so called Watts bath, composed of 300 g/L $CoSO_4$ $7H_2O$ (Sigma Aldrich ≥ 99,0%), 45 g/L $CoCl_2$ $6H_2O$ (Sigma Aldrich ≥ 99,0%); 45g/L H_3BO_3 (Sigma Aldrich ≥ 99,5%) was employed to perform cobalt electrodeposition, while, the same concentration of the analogue nickel salts were used during nickel nanowires electrodeposition. Metal electrodeposition was conducted by a pulsed electrodeposition. After electrodeposition template was selectively etched in 6M NaOH to obtain an array of free-standing metal nanowires. Metal loading was estimated by atomic adsorption spectroscopy (AAS, contrAA 300 – Analytik Jena AG) after electrode leaching in aqua regia. Field emission scanning electron microscopy (SEM, Zeiss Auriga) was employed to characterize the morphology and size of NWE electrodes. Focused ion beam (FIB, Orsay Physics - Cobra Ga column) was used to generate electrode cross sections. The chemical composition of the electrodes was determined by energy dispersive X-ray spectroscopy (EDX, Bruker QUANTAX 123 eV). The surface atomic composition of samples was analyzed by X-ray Photoelectron Spectroscopy (XPS, Omicron NanoTechnology MXPS system). The amount of CoO in CoNWs electrode was computed by merging the results of AAS, EDX and XPS analyses. EDX analysis showed that the amount of oxygen and cobalt in the cobalt nanowires was 23±2at.% and 77±12at.%, respectively, while XPS analysis showed that the $Co(OH)_2$ to CoO ratio was equal to 6.5±0.7. Taking into account the errors associated with each analysis, the maximum amount of CoO on the electrode could be estimated around 10% of the total cobalt mass determined by AAS.

Electrochemical characterizations

CoNWs as anode in lithium battery

Electrochemical impedance spectroscopy (EIS) tests were performed using a three-electrode polypropylene T-cell, with the CoNWs employed as working electrode, and two lithium disks employed as counter and reference electrode. Two Whatman glass fiber membranes were used to separate the anodic and the cathodic side. Commercial 1 M $LiPF_6$ in 1:1 v/v ethylene carbonate : dimethyl carbonate solution (Solvionic) was used as electrolyte. Each cell was assembled in an argon-filled glove box with a content of O_2 and H_2O less than 1 ppm. Galvanostatic tests were performed using Maccor Series 4000 Battery Test System (Maccor Inc.).

NiNWs symmetric supercapacitor:

Cyclic voltammetry (CV) measurements were conducted with a jacketed three electrode cell using an IVIUMnSTAT potentiostat. NiNWs electrode with an exposed surface area of 0.5 cm^2, platinum wire and Ag/AgCl were used as working, counter and reference electrode respectively. KOH 1M was the electrolytic solution. All the experiments were conducted at 25°C.

RESULTS AND DISCUSSION

CoNWs as anode in lithium battery

SEM characterization of electrodeposited alumina template showed a compact and ordered cobalt nanowire arrays on the electrode surface with a density of 10^{10} nanowires cm^{-2} (Fig.1-A). Cobalt nanowires extend from the bottom side to about half of the template length (Fig.1 B-C). In order to estimate the cobalt oxidation state and the presence of cobalt oxides, XPS analyses were performed.

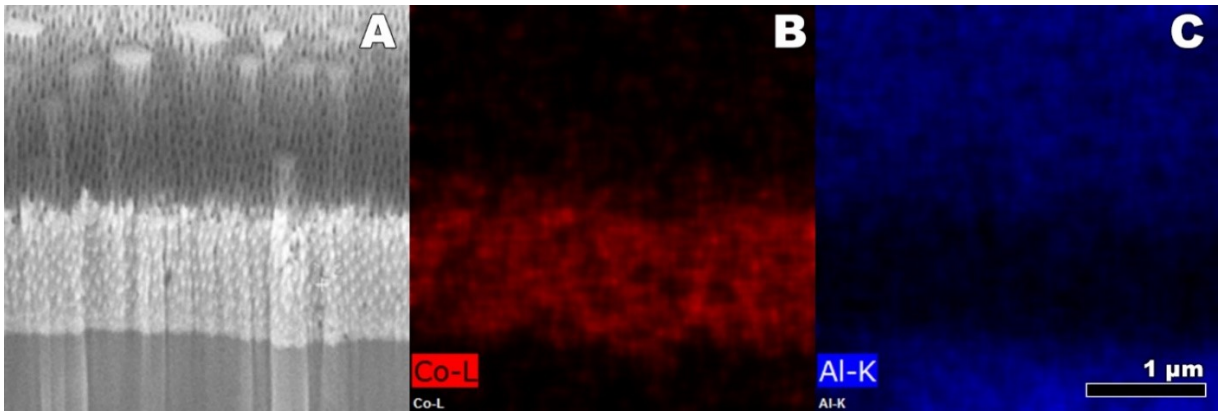

Figure 1. A) SEM cross sectional image after electrode milling by FIB. Cobalt (B) and aluminium (C) EDX mapping of milled electrode.

Fig. 2 shows XPS surface analysis results after the complete removal of template. XPS spectra shows the presence of a metallic Co component (eV 779 ca.) in addition to the largely prevailing Co^{2+} hydroxide/oxide contribution at higher binding energies (Fig.2)[11]. In order to estimate the effect of cobalt metallic core, a CoNWs electrode was thermally oxidized at 500°C for 4 hours. XPS of oxidized electrode displays the presence of lower satellite structures (eV 788 ca.) relative to Co^{2+} indicating the presence of Co^{3+}. Furthermore, the main peak with eV attributable to metallic Co, which was found in the pristine electrode, disappeared on the oxidized electrode[12].

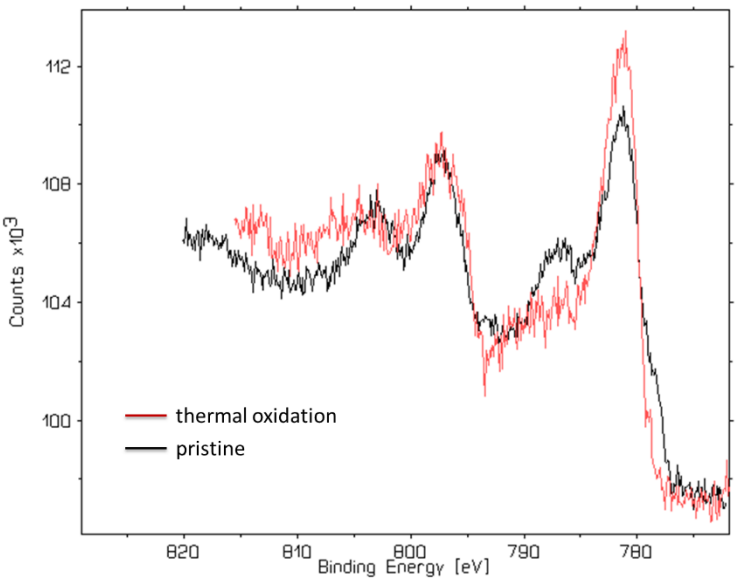

Figure 2. Co 2p monochromated XPS spectra related to pristine (black line) and after thermal oxidation of electrode (red line).

Both pristine (PE) and oxidized (TE) electrodes were tested as anode in a half-lithium cell for lithium storage evaluation. Li storage reaction involving nanosized CoO can be described as follows [5]:

$$CoO + 2Li \leftrightarrows Li_2O + Co \qquad (1)$$

It must be remarked that the reduction of Li_2O to Li showed in reaction 1 can occur only using nanosized active material [5]. Otherwise, Li_2O becomes inactive following its formation and reaction 1 is irreversible. Considering the reported storage reaction, the theoretical specific capacity of PE is 716 $mAhg^{-1}$ about two-times higher as compared to the most commonly used graphite anode capacity (372 $mAhg^{-1}$). Fig.3 shows the galvanostatic cycling performance of PE electrode at 2 Ag^{-1} (3.8 C). Remarkably, a capacity increase was observed during the initial 40 cycles and a practical capacity of 1700 $mAhg^{-1}$ after 100 cycles was obtained. The increased capacity as compared to the theoretical value of the PE electrode can be justified by pseudo-capacitance effects. These effects commonly recur on high surface area electrodes, and they feature, in general, all the nanostructured materials[13]. Fig.3 also includes the cycling performance of the TE electrode. A mean capacity of 800 $mAhg^{-1}$ was recorded on the first 10 cycles followed by a significant capacity fading until to 150 $mAhg^{-1}$ after 100 cycles. As it can be seen, a lower initial specific capacity with respect to the PE electrode was found. This result can be ascribed to a decrease in the surface area after the thermal oxidation, which determines the loss of the previously found extra-capacity contribution. As result, a practical capacity close to the theoretical capacity of Co_3O_4 was found (892 mAh g^{-1}). It is worth noting that the capacity fading during the galvanostatic cycling of TE electrode corroborate the hypothesis that an inactive metallic core improves cycle stability acting as a stable scaffold of the nanowires array electrode [1][3].

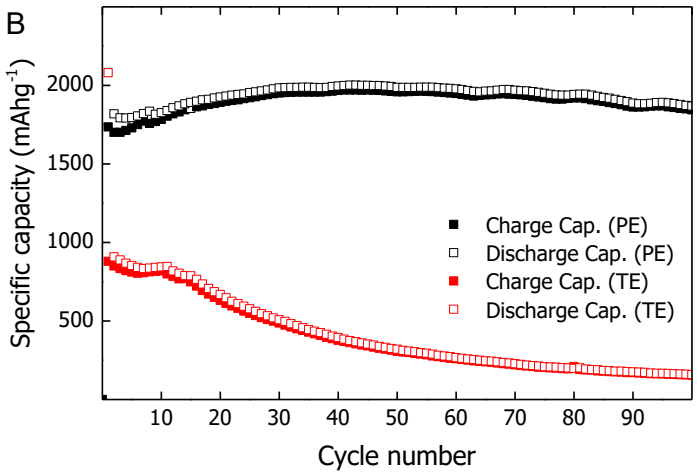

Figure 3. Cycling performance at 2 A g^{-1} (3.8 C) between 0.01-3 V.

NiNWs symmetric supercapacitor

Figure 4 shows the NiNWs electrode after alumina template removal. An ordered nickel nanowires structure was obtained with a total length of 3 µm. XPS surface analysis (Fig.5) of the electrode reveals that an oxide layer is formed covering the electrode obtained by dissolving the alumina template after the electrodeposition process. To investigate the composition of the oxide shell XPS O 1s spectra was analysed [14]. As shown in Figure 5 both NiOH (eV 531) and NiO (eV 528) was found on NiNWs with a ratio NiOH/NiO equal to 5.

Figure 4. Cross sectional SEM image of NiNWs electrode after alumina template dissolution. The produced NiNWs electrode was directly tested as supercapacitor electrode.

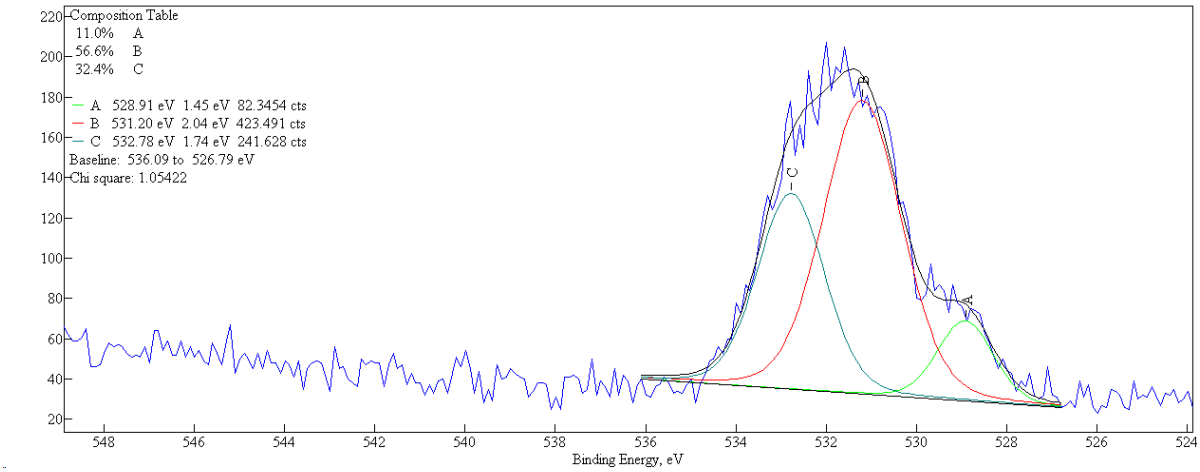

Figure 5. XPS O 1s region from NiNWs electrode.

A supercapacitor was assembled using the obtained electrode as working electrode in a three-electrode cell configuration. Figure 6-A shows the cyclic voltammograms obtained at different scan rate between 0.5 to 0 V vs Ag/AgCl. Cyclic voltammetry curves reveal two peaks both in the cathodic and anodic scan. During the cathodic scan

(50 mVs^{-1}), the two peaks recurring at 0.2 V and 0.12 V can be ascribed to the following reductions of NiOOH to NiO (Eq. 2) and $NiOH_2$ (Eq. 3), respectively [15]:

$$NiOOH + e^- \rightleftharpoons NiO + OH^- \quad (2)$$

$$NiOOH + e^- + H_2O \rightleftharpoons Ni(OH)_2 + OH^- \quad (3)$$

During the oxidation scan, a current increase was found at 0.4 V due to H_2O formation (4). This sharp current increase at low overpotentials with respect to the standard redox potential could indicate that OH^- oxidation was catalyzed by NiNWs electrode [16].

$$4\,OH^- \rightarrow O_2 + 2H_2O + 4e^- \quad (4)$$

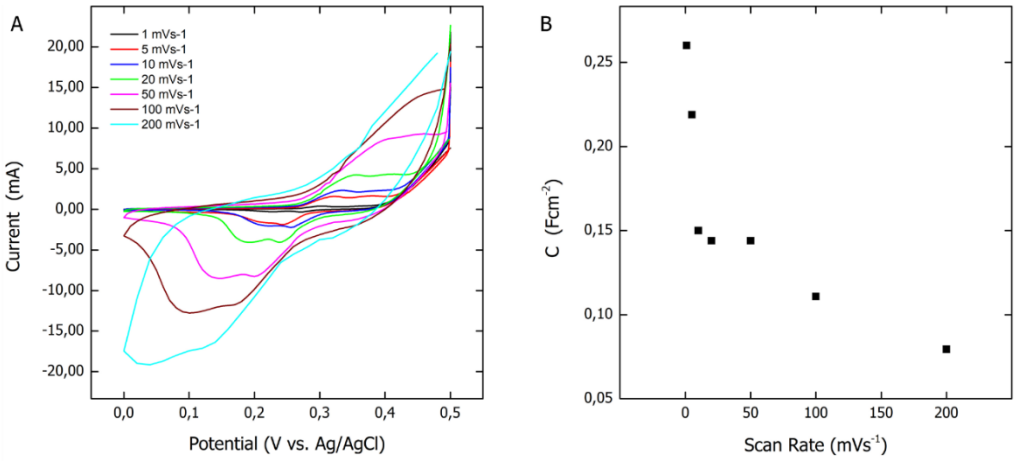

Figure 6. Cyclic voltammograms at various scan rate (A) and capacity values obtained at different scan rate (B).

The obtainment of faradaic peaks suggested the occurrence of pseudo-capacitive phenomena that recur at the surface of the nanowires. Figure 6-B and Table 1 report the obtained capacity estimated from voltammetric curves as follow:

$$C = \frac{1}{Av(V_c - V_a)} \int_{V_a}^{V_c} i(V)dV \quad (5)$$

Where A is the electrode geometric surface area, v the scan rate, $V_c - V_a$ the cell voltage and i the current.
Computed capacities in the scan rate range of 10-50 mVs^{-1} were almost constant with a mean value of 0.15 Fcm^{-2} while the higher and lower values were found respectively at the lower and higher scan rate.

TABLE 1: Computed and literature capacities values for $Ni(OH)_2$ based pseudocapacitor

Scan Rate (mVs^{-1})	Capacity (Fcm^{-2})	
	This work	**Li et al (2013)[17]**
1	0.26	0.262
5	0.22	0.200
10	0.15	0.178
50	0.14	0.150
100	0.11	
200	0.08	

CONCLUSIONS

Major advantage of the proposed electrochemical synthesis, as compared to alternative template electrodeposition methods, is that it can be implemented with one-side open alumina templates generated by one-step anodization of aluminum, thus excluding the application and coating of alumina membranes by metal sputter deposition. Further, electrodeposition allows directly obtaining metal oxide/hydroxide core shell nanowires, ruling out the separate reduction of the metal oxide nanowires which is required by the hydrothermal synthesis route.
These advantages lead to outstanding electrochemical performances that can be summarized as follow:
- The metallic core, obtained by template electrodeposition, ensure the CoNWs electrode stability when used as anode in a lithium cell. The capacity fading during the galvanostatic cycling of TE electrode corroborate the hypothesis that an inactive metallic core improves cycle stability acting as a stable scaffold of the nanowires array electrode
- Owing to the high surface area, the produced CoNWs electrode exhibits a reversible extra-capacity that can be imputed to pseudo-capacitance effects.
- During the nickel electrodeposition, a NiO-$NiOH_2$ shell is spontaneously formed over the surface of nickel nanowires under room conditions.
- The electrochemical characterization of the NiO-$NiOH_2$ capacitor showed a capacity close to the best literature value.
These advantages and the outstanding electrochemical performances achieved by the produced electrodes constitute fundamental pre-requisites towards the scale-up of the proposed method.

REFERENCES

1. Palacín, M.R. and A. de Guibert. Science **351**, 1253292 (2016).
2. Zhan, L., S. Wang, L.-X. Ding, Z. Li, and H. Wang. Journal of Materials Chemistry A **3**, 19711-19717 (2015).
3. Schiavi, P.G., L. Farina, R. Zanoni, P. Altimari, I. Cojocariu, A. Rubino, M.A. Navarra, S. Panero, and F. Pagnanelli. Electrochim. Acta **319**, 481-489 (2019).
4. Fu, Y., X. Li, X. Sun, X. Wang, D. Liu, and D. He. J. Mater. Chem. **22**, 17429-17431 (2012).
5. West, W.C., N.V. Myung, J.F. Whitacre, and B.V. Ratnakumar. J. Power Sources **126**, 203-206 (2004).
6. Jang, B., E. Pellicer, M. Guerrero, X. Chen, H. Choi, B.J. Nelson, J. Sort, and S. Pané. ACS Applied Materials & Interfaces **6**, 14583-14589 (2014).
7. Schiavi, P.G., P. Altimari, F. Pagnanelli, E. Moscardini, and L. Toro. Chemical Engineering Transactions **43**, 673-678 (2015).
8. Schiavi, P.G., P. Altimari, A. Rubino, and F. Pagnanelli. Electrochim. Acta **259**, 711-722 (2018).
9. Schiavi, P.G., A. Rubino, P. Altimari, and F. Pagnanelli. *Two electrodeposition strategies for the morphology-controlled synthesis of cobalt nanostructures*. in *AIP Conference Proceedings*. 2018.
10. Cheng, W., M. Steinhart, U. Gösele, and R.B. Wehrspohn. J. Mater. Chem. **17**, 3493-3495 (2007).
11. Schiavi, P.G., P. Altimari, R. Zanoni, and F. Pagnanelli. Electrochim. Acta **220**, 405-416 (2016).
12. Yang, J., H. Liu, W.N. Martens, and R.L. Frost. The Journal of Physical Chemistry C **114**, 111-119 (2009).
13. Schiavi, P.G., L. Farina, P. Altimari, M.A. Navarra, R. Zanoni, S. Panero, and F. Pagnanelli. Electrochim. Acta **290**, 347-355 (2018).
14. Marrani, A.G., V. Novelli, S. Sheehan, D.P. Dowling, and D. Dini. ACS Applied Materials & Interfaces **6**, 143-152 (2014).
15. Srinivasan, V. and J.W. Weidner. J. Electrochem. Soc. **147**, 880-885 (2000).
16. Du, P., R.J.E. Eisenberg, and E. Science. **5**, 6012-6021 (2012).
17. Li, H.B., M.H. Yu, F.X. Wang, P. Liu, Y. Liang, J. Xiao, C.X. Wang, Y.X. Tong, and G.W. Yang. Nature Communications **4**, 1894 (2013).